

# Reduction of platinum dispersed on dealuminated beta zeolite

Ling-Wen Ho<sup>a</sup>, Chin-Pei Hwang<sup>a</sup>, Jyh-Fu Lee<sup>c</sup>, Ikai Wang<sup>b</sup>, Chuin-Tih Yeh<sup>a,\*</sup>

<sup>a</sup> Department of Chemistry, National Tsing-Hua University, Hsinchu 30043, Taiwan

<sup>b</sup> Department of Chemical Engineering, National Tsing-Hua University, Hsinchu 30043, Taiwan

<sup>c</sup> Synchrotron Radiation Research Center, No. 1 R & D Road VI, Hsinchu Science-Based Industrial Park, Hsinchu 30043, Taiwan

Received 25 July 1997; accepted 10 February 1998

## Abstract

The Si/Al ratio of a commercial HB-25 beta zeolite sample was increased by treatment of dealumination and silicon-insertion. Platinum ions were subsequently dispersed onto the starting and the treated samples through impregnation of aqueous  $\text{Pt}(\text{NH}_3)_4(\text{NO}_3)_2$ . Chemical environments of dispersed platinum were characterized by temperature-programmed reduction (TPR) technique. The obtained TPR traces varied with extents of dealumination. Nevertheless, three major signals, in reduction temperature regions around  $-50$ ,  $80$  and  $480^\circ\text{C}$  were distinguished from these TPR traces and characterized as reductions of platinum oxides dispersed on the external surface of zeolite ( $\text{Pt}^\circ\text{O}$ ), platinum oxides occluded in channels ( $\text{Pt}^\circ\text{O}_x$ ), and  $\text{Pt}-(-\text{O}-\text{Si}\equiv)_y$  complexes coordinated to external surface or defects of zeolite, respectively. From the variation in the contribution of the  $480^\circ\text{C}$  peak in TPR traces, a formation of Si–OH silanol function groups on the zeolite surface during the dealumination treatment and a elimination of these groups during the silicon-insertion treatment are indicated. © 1998 Elsevier Science B.V. All rights reserved.

**Keywords:** TPR; Platinum oxide; Beta zeolite; Dealumination

## 1. Introduction

Pores in the beta and the KL zeolites are straight channels of 12-member ring. The KL zeolite has a Si/Al atomic ratio around 3.0 and unidimensional channels of 0.71 nm in diameter [1]. The beta zeolite is a three dimensionally interconnected channel system which has a high Si/Al ratio ( $> 10$ ) and an extensively faulted structure [2,3]. Both zeolites are widely used in industrial processes after impregnation with Pt. The Pt/KL catalyst exhibits a good selectivity

for the aromatization of *n*-hexane [4,5], while the Pt/beta catalyst is an active bifunctional catalyst towards reforming and isomerization reactions [6,7].

The acidic strength of aluminum sites in a zeolite generally increases with its Si/Al ratio. The Si/Al ratio of a zeolite can be increased by treatments of either dealumination with inorganic acid ( $\text{HNO}_3$  or  $\text{HCl}$  solution) [8], or silicon-insertion with  $(\text{NH}_4)_2\text{SiF}_6$  [9]. During the acid treatment, aluminum ions are leached out and defective vacancies as well as terminal Si–OH groups are consequently formed on the framework of zeolite. The resulted defects and

\* Corresponding author. Fax: 886-3-5711082.

Table 1  
Some literatures about TPR of Pt/zeolites

Sample	$T_r$ (°C)	Pt species	Ref. [precursor]
Pt/Y	100	Pt <sup>2+</sup> in supercage	[10] [Pt(NH <sub>3</sub> ) <sub>4</sub> (NO <sub>3</sub> ) <sub>2</sub> ]
	250	Pt <sup>4+</sup> in sodalite cage or hexagonal prism	[11] [Pt(NH <sub>3</sub> ) <sub>4</sub> Cl <sub>2</sub> ]
Pt/ZSM-5	250	Pt <sup>4+</sup> in channels	[11] [Pt(NH <sub>3</sub> ) <sub>4</sub> Cl <sub>2</sub> ]
Pt/KL	r.t.	PtO on external surface	[11,12] [Pt(NH <sub>3</sub> ) <sub>4</sub> Cl <sub>2</sub> ]
	80	PtO in channels	
	150	Pt <sup>2+</sup> in channels	
	250	Pt <sup>4+</sup> in channels	

terminal Si–OH groups may be partially removed by an additional treatment of silicon-insertion.

The temperature-programmed reduction (TPR) technique has been used successfully in literature (see Table 1) to characterize environments of Pt species supported on Y, ZSM-5 and L zeolites according to their reduction temperature ( $T_r$ ) [10,12]. Sachtler et al. [10] and Fogar and Jaeger [11] found that, platinum ions in the supercage of Y zeolite were reduced at a lower temperature ( $T_r = 100^\circ\text{C}$ ) than those in the sodalite cage or in the hexagonal prism ( $T_r = 250^\circ\text{C}$ ). Recently, four different Pt species, i.e., PtO deposited on external surface ( $T_r < 25^\circ\text{C}$ ), PtO occluded in channels ( $T_r = 80^\circ\text{C}$ ), Pt<sup>2+</sup> coordinated to the framework ( $T_r = 150^\circ\text{C}$ ) as well as a coordinated Pt<sup>4+</sup> species ( $T_r = 250^\circ\text{C}$ ) were further distinguished from Pt/KL zeolite samples [11,12].

In this work, platinum ions dispersed on beta zeolite are characterized by TPR. We want to report that defect sites formed during dealumination of the zeolite have a profound effect on the reduction of impregnated platinum.

## 2. Experimental

### 2.1. Dealumination of beta zeolite

The commercial (PQ Corporation) HB-25 beta zeolite (Si/Al atomic ratio = 11) was used

as the starting zeolite sample in this work. This sample was dealuminated by stirring in a 1 M HNO<sub>3</sub> solution at room temperature for 3 days. The aluminum-leached sample was subsequently filtrated, washed with deionized water, dried overnight at 110°C, calcined in air at 540°C for 5 h and named as HB-N.

### 2.2. Insertion of silicon

Part of the HB-N sample prepared was further treated with a silicon-insertion agent. In this insertion, 15 ml of a 0.3 M aqueous (N-H<sub>4</sub>)<sub>2</sub>SiF<sub>6</sub> solution was added dropwise into 5 g of the HB-N sample suspended in an aqueous solution of ammonium acetate (50 ml, 2 M) at a temperature of 90°C. After filtration, washing, drying and calcination treatments, the resulted sample was stored as HB-NS.

Calcined HB-N and HB-NS maintained their beta structure according to XRD characterizations.

### 2.3. Platinum impregnation

Supported platinum samples were prepared by the incipient-wetness impregnation of HB, HB-N and HB-NS zeolites with a 0.023 M Pt(NH<sub>3</sub>)<sub>4</sub>(NO<sub>3</sub>)<sub>2</sub> aqueous solution. After an overnight drying at 110°C, the impregnated samples were calcined at 400°C for 3 h and named as Pt/HB, Pt/HB-N, Pt/HB-NS, respectively.

### 2.4. Preparation of Pt/SiO<sub>2</sub>

Two kinds of Pt/SiO<sub>2</sub> samples were prepared for this study. One was prepared by impregnating Carbosil M-5 powders (S.A. = 200 m<sup>2</sup> g<sup>-1</sup>) with an aqueous PtCl<sub>4</sub> solution. The other was prepared through sol–gel method by mixing Pt(NH<sub>3</sub>)<sub>4</sub>(NO<sub>3</sub>)<sub>2</sub> (in 1 N NaOH) with Si(OC<sub>2</sub>H<sub>5</sub>)<sub>4</sub> in (EtOH/NaOH). After evaporation at 110°C, the obtained solid samples were calcined at 500°C for 4 h and named as Pt/SiO<sub>2</sub>(i) and Pt/SiO<sub>2</sub>(g).

## 2.5. ICP measurements

After a 2 h dehydration at 200°C, part of each prepared sample was dissolved in a mixed solution of HF and aqua regia at 120°C for composition determinations. The bulk Si/Al ratios were determined by a Jarrell-Ash, ICAP 9000 ICP/AES. Loadings of platinum impregnated on the zeolite samples were analyzed by a Kontron, S-35 ICP/MS.

## 2.6. $^{29}\text{Si}$ MAS NMR characterization

$^{29}\text{Si}$  MAS NMR spectra for all of the beta zeolites used were obtained from a Bruker MSL-200 spectrometer at an operating frequency of 39.73 MHz. A 3000 Hz magic angle spinning was performed during the signal collection. Reported chemical shifts were related to a standard of  $\text{Si}(\text{CH}_3)_4$ .

## 2.7. TPR measurements

TPR studies were performed in an apparatus described in a previous report [13]. A 30 ml  $\text{min}^{-1}$  flow of 10 vol.%  $\text{H}_2$  in Ar was used as the reductive gas. The rate of hydrogen consumption was monitored by a thermal conductivity detector on raising the sample temperature from  $-80$  to  $700^\circ\text{C}$  at a constant rate of  $7^\circ\text{C min}^{-1}$ .

## 2.8. X-ray absorption spectroscopy

X-ray absorption spectra were recorded at the wiggler beamline S-5B of Synchrotron Radiation Research Center, Taiwan. The monochromator employs double Si(111) crystals for energy scanning. Powdered sample was pressed into a stainless steel holder and measured at liquid nitrogen temperature. A transmission mode was selected in which the intensities of incident and transmitted beams were measured using gas ionization chambers. Three scans were averaged to increase the signal-to-noise ratio. The computer software for data analysis was implemented in UWXAFS 3.0 package [14] in which the phase shift and backscattering amplitude of the photoelectron wave were theoretically calculated by using FEFF 6 code [15,16].

## 3. Results and discussion

### 3.1. Composition of Pt/beta samples

The analyzed Si/Al ratios of the starting (HB-25), dealuminated (HB-N) and Si-inserted (HB-NS) beta zeolites are seen in Table 2 to increase from 11 of the HB-25 to 90 of the HB-N and 127 of the HB-NS. Over 80% of Al atoms was removed from the starting beta zeolite by the dealumination treatment. Besides the expected silicon insertion, part of the aluminum ions remained in the HB-N sample was additionally removed in the Si-insertion treatment

Table 2  
Compositions and TPR results of Pt samples prepared in this study

	ICP/AES		TPR (area %)				
	Si/Al ratio	Pt (wt.%)	$-50^\circ\text{C}$	$80^\circ\text{C}$	$250^\circ\text{C}$	$480^\circ\text{C}$	$N_{\text{H}}/N_{\text{Pt}}$
Pt/SiO <sub>2</sub> (i)	$\alpha$	0.81	100	—	—	—	0.8
Pt/HB	11	0.39	35.1	3.8	3.0	58.1	2.0
Pt/HB-N	90	0.35	11.3	—	2.9	85.7	2.9
Pt/HB-NS	127	0.34	84.4	—	—	15.6	1.2
Pt/SiO <sub>2</sub> (g)	$\alpha$	0.47	—	—	—	100	3.8

[9]. The platinum content in the three platinum impregnated samples was shown to be around 0.35 wt.% according to measurements by ICP/MS (Table 2).

### 3.2. $^{29}\text{Si}$ MAS NMR

Fig. 1 shows the  $^{29}\text{Si}$  MAS NMR spectra of three beta zeolites used in this report. A major peak at  $\sim -110$  ppm and a shoulder peak at  $-105$  ppm were found in trace a from the fresh beta zeolite. They can be assigned to Si (0 Al) and Si (1 Al), respectively [17]. After acid treatment, the Si (1 Al) shoulder peak disappeared (trace b). In its replacement, a minor peak at  $-102$  ppm appeared. This peak has been assigned by Corma et al. [18] to silicon atoms bonded to a hydroxyl group. Conceivably, the broad peak around  $-102$  ppm is assigned to SiOH groups of hydroxyl nests

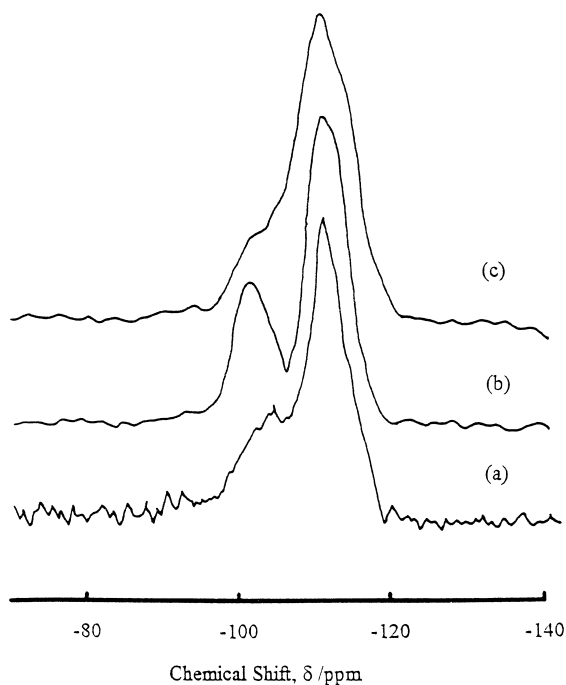


Fig. 1.  $^{29}\text{Si}$  MAS NMR of (a) HB-25; (b) HB-N; (c) HB-NS.

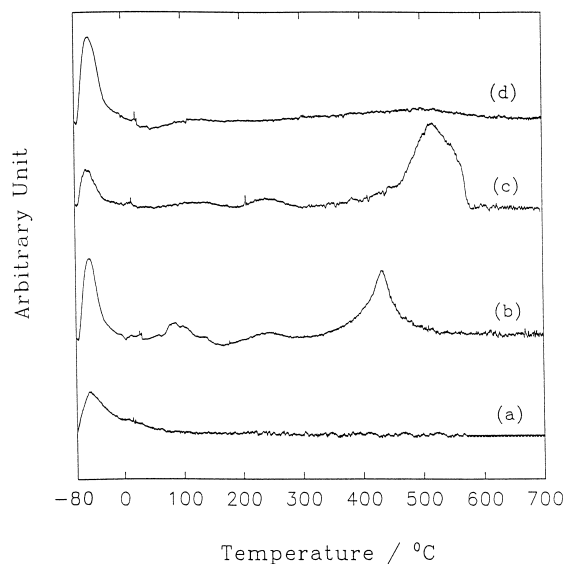
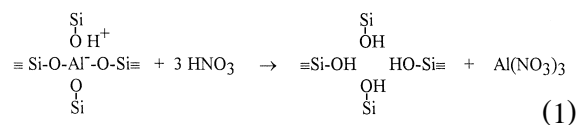
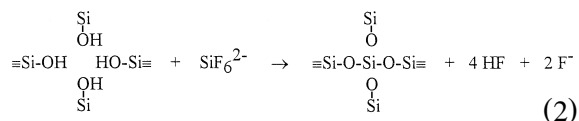


Fig. 2. TPR diagrams of (a) Pt/SiO<sub>2</sub>(i); (b) Pt/HB; (c) Pt/HB-N; (d) Pt/HB-NS.

formed during the following dealumination reaction [19]:



The peak at  $-102$  ppm diminished after silicon insertion (HB-NS sample) (trace c). Evidently, most of the SiOH groups on HB-N sample was removed by the following reaction:



### 3.3. TPR of Pt / beta samples

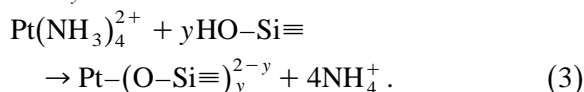
Fig. 2 shows the TPR traces of four Pt samples prepared. These traces are composed of four reduction peaks, with  $T_r = -50$ , 80, 250 and around  $480^\circ\text{C}$ , respectively. Their relative areas in these traces are also listed in Table 2.

The Pt/SiO<sub>2</sub>(i) sample was prepared by impregnating a Pt complex onto the Carbosil M-5 support. This support is composed of highly

sintered silica grains (with diameters  $\sim 30$  nm) which do not contain any internal pore. The Pt species dispersed on the surface of these grains was reduced (in trace a of Fig. 2) exclusively at  $-50^\circ\text{C}$  [11]. Accordingly, the Pt species reduced at  $-50^\circ\text{C}$  in traces b, c and d of Pt/beta samples can also be assigned to Pt oxides deposited on the external surface of beta zeolite ( $\text{Pt}^\circ\text{O}$ ). The remaining three peaks, with  $T_r = 80$ , 250 and around  $480^\circ\text{C}$ , respectively, must have resulted from Pt species either occluded into the zeolite channels or coordinated to the surface of zeolites.

Recently, Sachtler et al. [12] characterized the Pt/KL samples by TPR. Besides the PtO on external surface, they found three other platinum species, i.e., PtO occluded in channels ( $T_r = 80^\circ\text{C}$ ),  $\text{Pt}^{2+}$  ( $T_r = 150^\circ\text{C}$ ) and  $\text{Pt}^{4+}$  ( $T_r = 250^\circ\text{C}$ ) ions, respectively. Two of these peaks with  $T_r = 80$  and  $150^\circ\text{C}$  are also observed in the trace b of Fig. 2 from the Pt/HB sample. However, the total contribution of these three peaks ( $< 10\%$ ) in trace b is much smaller than those found in the Pt/KL samples ( $> 80\%$  in total). The difference in contribution probably resulted from the difference in Si/Al ratio between the HB (Si/Al  $\sim 11$ ) and KL (Si/Al  $\sim 3$ ) zeolites.

The  $430^\circ\text{C}$  peak is a major peak in trace b of Pt/HB sample. This peak was observed in the Pt/KL and Pt/KB samples of Perez-Pariente et al. [20] and Zhang et al. [21]. In their reports, the peak with  $T_r = 430^\circ\text{C}$  was assigned to  $\text{Pt}^{2+}$  ions in some hidden sites. However, Treacy and Newsam [3] proposed that beta zeolite is a highly intergrown hybrid of two distinctive but closely related polymorphs (A and B) and contains a large population of stacking faults and terminal SiOH (silanol) groups. Accordingly, part of platinum complex ions on Pt/beta samples may coordinate to the silanol ( $\equiv\text{Si}-\text{OH}$ ) sites during impregnation to form  $\text{Pt}-(\text{O}-\text{Si}\equiv)_y^{2-y}$ :



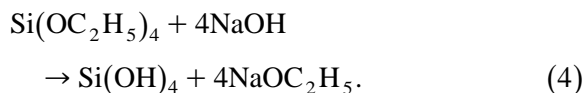
The observed  $430^\circ\text{C}$  peak is therefore attributed to a reduction of  $\text{Pt}-(\text{O}-\text{Si}\equiv)_y^{2-y}$  species formed in reaction 3.

During the dealumination treatment, the number of terminal Si-OH groups on beta zeolite should be increased due to a formation of Si-OH nests [22,23], through reaction 1. Platinum ions impregnated onto the HB-N sample therefore had a better chance to coordinate with the hydroxyl nests to form  $\text{Pt}-(\text{O}-\text{Si}\equiv)_y^{2-y}$ . This expectation is indeed confirmed by a dominant  $530^\circ\text{C}$  peak in trace c of Fig. 2. A large  $N_{\text{H}}/N_{\text{Pt}}$  ratio (2.9) shows that most of Pt ions in the nest has been oxidized into  $4+$  oxidation state during the calcination pretreatment. The notable variation in  $T_r$  (from  $430^\circ\text{C}$  to  $530^\circ\text{C}$ ) probably resulted from differences in the stoichiometry of  $y$  of reaction 3 and/or in the oxidation state ( $n$ ,  $4+$  or  $2+$ ) of Pt ions.

Most of the hydroxyl nests on HB-N should be eliminated during the Si-insertion treatment (reaction 2). In agreement to our expectation, the peak of  $\text{Pt}-(\text{O}-\text{Si}\equiv)_y^{n-y}$  suddenly became diminished in trace d for the Pt/HB-NS sample.

### 3.4. TPR of Pt/SiO<sub>2</sub>(g)

In order to prove that the structure of Pt species reduced around  $480^\circ\text{C}$  is  $\text{Pt}-(\text{O}-\text{Si}\equiv)_y^{n-y}$ , we specially prepared a Pt/SiO<sub>2</sub>(g) sample from gelating a Pt solution [ $\text{Pt}(\text{NH}_3)_4(\text{NO}_3)_2$ ] in the basic tetraethyl orthosilicate solution. In this basic solution,  $\text{Si}(\text{OC}_2\text{H}_5)_4$  would react with NaOH to form SiOH groups:



The SiOH groups formed should subsequently coordinate to Pt ions (reaction 3) to form  $\text{Pt}-(\text{O}-\text{Si}\equiv)_y^{4-y}$  complexes during the gelation and the calcination treatment. These Pt species were found reduced around  $550^\circ\text{C}$  in trace a of Fig. 3. Accordingly, the reduction peak between 400 and  $550^\circ\text{C}$  in Pt/beta zeolite samples can in-

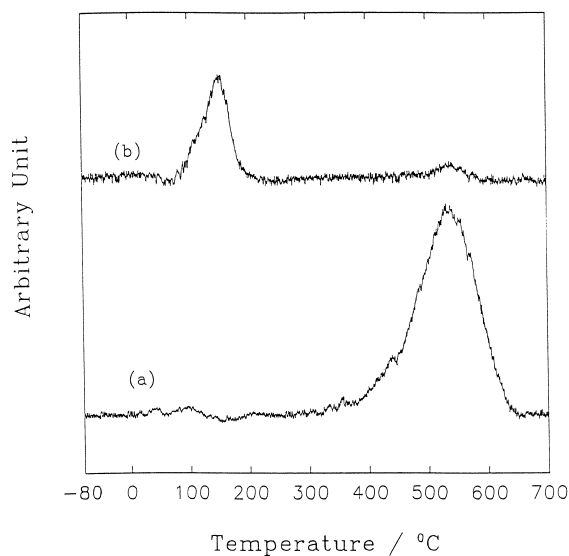
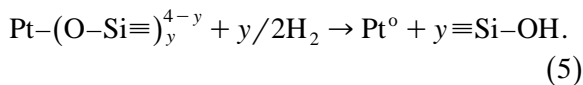


Fig. 3. TPR diagrams of Pt/SiO<sub>2</sub>(g): (a) fresh sample; (b) sample (a) reoxidized at 500 °C.

deed be assigned to the reduction of Pt-(O-Si≡)<sub>y</sub><sup>4-y</sup> species:



The oxidation state of Pt ions in this species is

in 4 + because the stoichiometry ( $N_{\text{H}}/N_{\text{Pt}}$ ) observed was 3.8 (Table 2).

After the experiment of trace a, the reduced Pt/SiO<sub>2</sub>(g) sample was reoxidized at 500°C for a second TPR experiment. Trace b of Fig. 3 indicated that the reduction of the reoxidized platinum on Pt/SiO<sub>2</sub>(g) was shifted to 130°C. Probably, the Pt<sup>0</sup> crystallites reduced in reaction 5 were incorporated in the bulk of SiO<sub>2</sub> support [24]. Therefore, the peak with  $T_r = 130^\circ\text{C}$  in the trace b should be the reduction of Pt oxides buried in the SiO<sub>2</sub> matrix.

### 3.5. Extended X-ray absorption fine structure (EXAFS) of Pt/SiO<sub>2</sub>(g)

After the background subtraction and normalization with respect to the edge jump step in the raw X-ray absorption spectra, the EXAFS function ( $\chi$ ) was obtained. Fig. 4 shows the  $k^3$ -weighted EXAFS function and its Fourier transform of the Pt/SiO<sub>2</sub>(g) sample. Computer-fitted results indicate that in average there are 3.5 nearest oxygen atoms surrounding each Pt atom

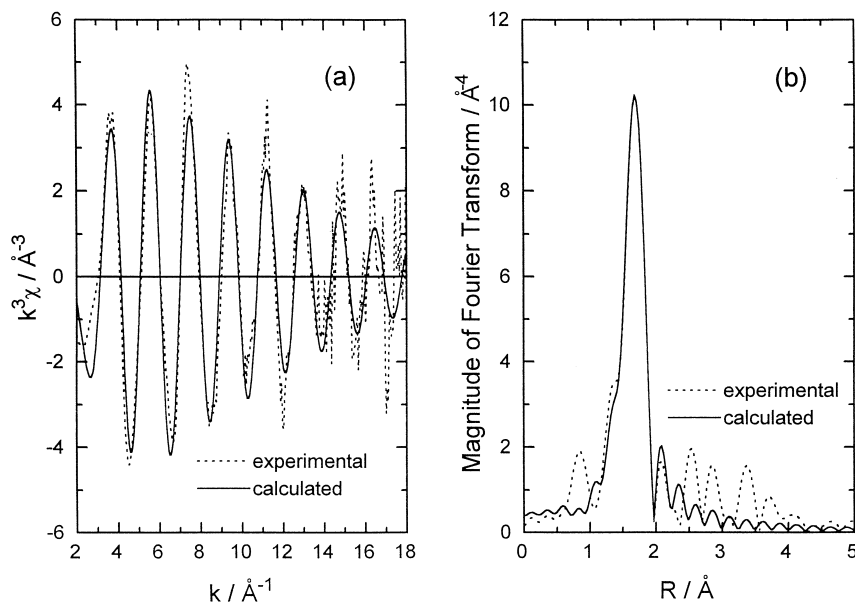


Fig. 4. (a)  $k^3$ -Weighted EXAFS function at Pt L<sub>3</sub>-edge of Pt/SiO<sub>2</sub>(g); (b) Magnitude of Fourier transform (without phase correction).

with a Pt–O bond length of 2.02 Å [14]. Taking into account the uncertainty in estimating the coordination number from EXAFS data analysis of  $\pm 15\%$ . Pt ions should locate at the center of a local oxygen tetrahedron, similar to the situation that the Si center is substituted by Pt in a  $\text{SiO}_4$  unit in gel structure. In view of the fact that the Pt/ $\text{SiO}_2(\text{g})$  sample exhibits no peak in XRD pattern due to the lack of long-range order, it becomes difficult to see the contribution in EXAFS from higher-shell neighbors surrounding the Pt center.

#### 4. Conclusions

Four kinds of TPR peaks were observed in Fig. 2 and assigned to reductions of the  $\text{Pt}^\circ\text{O}$  ( $T_r \sim -50^\circ\text{C}$ ), the  $\text{Pt}^\circ\text{O}_x$  ( $T_r = 80^\circ\text{C}$ ),  $\text{Pt}^{4+}$  ions in zeolite channels ( $T_r = 250^\circ\text{C}$ ), and species of  $\text{Pt}-(\text{O}-\text{Si}\equiv)_y^{n-y}$  in the defects of beta zeolite ( $T_r$  between 400 and  $550^\circ\text{C}$ ), respectively. The distribution of platinum in these environments can be estimated from the area of these peaks in TPR traces. Besides, a generation of Si–OH functional groups during the dealumination treatment and an elimination of these groups during the Si-insertion treatment was confirmed by variations in area of a TPR peak with  $T_r$  around  $480^\circ\text{C}$ . Accordingly, TPR technique can be used to characterize effects of dealumination treatments on zeolite structure.

#### Acknowledgements

The authors acknowledge the financial support of this study by the National Science Coun-

cil of the Republic of China under Contract No. NSC 86-2113-M-007-029.

#### References

- [1] R. Szostak, Handbook of Molecular Sieves, Van Nostrand-Reinhold, New York, 1992, pp. 274–277.
- [2] R. Benslama, J. Fraissard, A. Albizane, F. Fajula, F. Figueras, Zeolites 8 (1988) 196.
- [3] M.M. Treacy, J.M. Newsam, Nature 332 (1988) 249.
- [4] J.R. Bernard, in: Proceedings, 5th International Conference on Zeolites, Heyden, London, 1980, p. 66.
- [5] J. Zheng, J.L. Dong, Q.H. Xu, Y. Liu, A.Z. Yan, Appl. Catal. A: General 126 (1995) 141.
- [6] I. Wang, T.C. Tsai, S.T. Huang, Ind. Eng. Chem. Res. 29 (1990) 2005.
- [7] T.C. Tsai, I. Wang, Appl. Catal. 77 (1991) 199.
- [8] E.F.T. Lee, L.V.C. Rees, J. Chem. Soc., Faraday Trans. 1 83 (1987) 1531.
- [9] X. Liu, R. Xu, J. Chem. Soc., Chem. Commun. (1989) 1837.
- [10] S.H. Park, M.S. Tzou, W.M.H. Sachtler, Appl. Catal. 24 (1986) 85.
- [11] K. Foger, H. Jaeger, Appl. Catal. 56 (1989) 137.
- [12] D.J. Ostgard, L. Kustov, K.R. Poepelmeier, W.M.H. Sachtler, J. Catal. 133 (1992) 342.
- [13] C.P. Hwang, C.T. Yeh, J. Mol. Catal. A: Chemical 112 (1996) 295.
- [14] E.A. Stern, M. Newville, B. Ravel, Y. Yacoby, D. Haskel, Physica B 208 and 209 (1995) 117.
- [15] J.J. Rehr, R.C. Albers, S.I. Zabinsky, Phys. Rev. Lett. 69 (1992) 3397.
- [16] J.J. Rehr, Jpn. J. Appl. Phys. 32 (1993) 8.
- [17] C.A. Fyfe, Solid State NMR for Chemists, Chap. 7, Guelph, Ontario, Canada NIA 6Z9, 1983.
- [18] A. Corma, V. Fornes, J.B. Monton, A.V. Orchilles, J. Catal. 107 (1987) 288.
- [19] G.C. Bond, M.R. Gelsthorp, Appl. Catal. 35 (1987) 169.
- [20] J. Perez-Pariente, J. Sanz, V. Fornes, A. Corma, J. Catal. 124 (1990) 217.
- [21] J. Zhang, J.L. Dong, Q.H. Xu, Stud. Surf. Sci. Catal. 84 (1994) 1641.
- [22] J. Zhang, J.L. Dong, Q.H. Xu, C. Hu, Catal. Lett. 37 (1996) 25.
- [23] E. van Steen, G.S. Sewell, R.A. Makhothe, C. Micklethwaite, H. Manstein, M. de Lange, C.T. O'Connor, J. Catal. 162 (1996) 220.
- [24] J. Biswas, I.E. Maxwell, Appl. Catal. 63 (1990) 197.